ACS APPLIED MATERIALS & INTERFACES

Research Article

www.acsami.org

Ultrasound Responsive Macrophase-Segregated Microcomposite Films for *in Vivo* Biosensing

Jian Yang,[†] James Wang,[‡] Casey N. Ta,[§] Erin Ward,[∥] Christopher V. Barback,[⊥] Tsai-Wen Sung,[‡] Natalie Mendez,[#] Sarah L. Blair,*[,∥] Andrew C. Kummel,*[,†] and William C. Trogler*[,†]

[†]Department of Chemistry and Biochemistry, [‡]Department of Nanoengineering, [§]Department of Computer, [∥]Department of Surgery, [⊥]Department of Radiology, and [#]Materials Science and Engineering Program, University of California, San Diego, 9500 Gilman Drive, La Jolla, California 92093, United States

Supporting Information

ABSTRACT: Ultrasound imaging is a safe, low-cost, and *in situ* method for detecting *in vivo* medical devices. A poly(methyl-2-cyanoacrylate) film containing 2 μm boron-doped, calcined, porous silica microshells was developed as an ultrasound imaging marker for multiple medical devices. A macrophase separation drove the gas-filled porous silica microshells to the top surface of the polymer film by controlled curing of the cyanoacrylate glue and the amount of microshell loading. A thin film of polymer blocked the wall pores of the microshells to seal air in their hollow core, which served as an ultrasound contrast agent. The ultrasound activity disappeared when curing conditions were modified to prevent the macrophase segregation. Phase segregated films were attached to multiple surgical tools and needles and gave strong color Doppler signals *in vitro* and *in vivo* with the use of a clinical ultrasound imaging instrument. Postprocessing of the simultaneous color Doppler and B-mode images can be used for autonomous identification of implanted surgical items by correlating the two images. The thin films were also hydrophobic, thereby extending the lifetime of ultrasound signals to hours of imaging in tissues by preventing liquid penetration. This technology can be used as a coating to guide the placement of implantable medical devices or used to image and help remove retained surgical items.

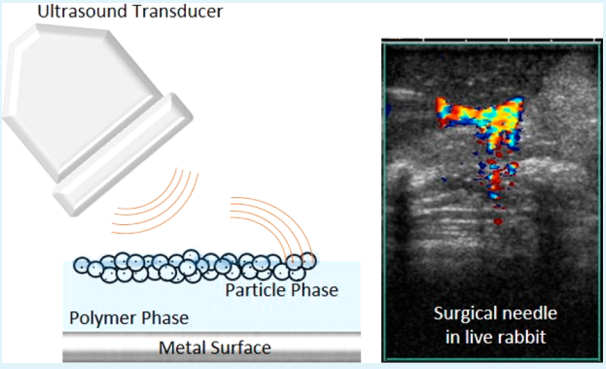

KEYWORDS: *silica microshells, cyanoacrylate, macrophase segregated film, ultrasound imaging, in vivo medical devices*

INTRODUCTION

Biomedical devices such as needles, catheters, biopsy markers, and guidewires are used widely in the health care field.[1−3] Biomedical devices are often composed of materials such as stainless steel, titanium, silicon, and polymers.[4] These devices may be implanted within complex physiological environments such as the abdominal cavity, gastrointestinal lumen, or the cardiovascular system. At present, physicians rely on medical imaging modalities, such as ultrasound, X-ray, and CT scans, to monitor or detect implanted biomedical tools during and after a procedure. Many procedures require precision; for example, to successfully achieve a nerve block, a physician must accurately inject local anesthesia to the target nerve bundles while avoiding surrounding blood vessels and other tissue structures.[5] To minimize the chance of unintentionally damaging surrounding nerves, blood vessels, and tissues while achieving the goal of attaining a nerve block, the needle entry and path through the tissue must be precise. Successful injection of the target area depends greatly on the experience of the medical professional.[6] In order to improve the injection accuracy, ultrasound (US) guided needle injection technology was developed and is now widely used in a variety of medical and surgical procedures. Ultrasound guidance is used for needle biopsies and epidurals and to allow physicians to safely place central venous and arterial catheters. While conventional B-mode ultrasound imaging helps visualize a needle during its approach toward the target tissue,[7] B-mode ultrasound has several limitations. For instance, B-mode ultrasound exhibits interfering signals due to scattering by various tissues or implants.[8] In light of such limitations, it was postulated that it may be beneficial to develop an ultrasound based platform based on high contrast ultrasound imaging modes, such as color Doppler or contrast-enhanced ultrasound, and apply it to positioning and monitoring implantable biomedical devices.

Detection of retained surgical items (RSI) in the operating room is another challenge for biomedical imaging technology. Small surgical items such as surgical needles, forceps, sutures, and blades can be accidentally left in patients' bodies after an operation. This may cause adverse consequences such as organ damage, bowel perforation, severe pain, sepsis, and even death.

Received: August 26, 2016
Accepted: December 21, 2016
Published: December 21, 2016

DOI: 10.1021/acsami.6b10728
ACS Appl. Mater. Interfaces 2017, 9, 1719−1727

Scheme 1. Macrophase Separation of PMCA/Microshells Composite during Curing[a]

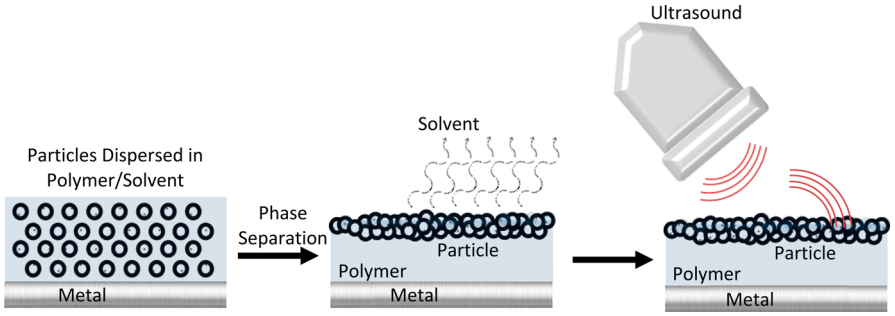

[a]Air-filled silica shells were driven to the surface of the polymer matrix and covered by a thin polymer film to trap air in the shells when a solvent was added to slow the rate of curing. This made the film visible by ultrasound.

It has been estimated that up to 2000 cases of RSI occur in the United States each year.[9] A routine surgical tool count is the most commonly used method to prevent RSI from occurring.[10] Radio-frequency (RF) tags attached to large surgical items, such as sponges and gauges, can be detected by a RF reader and help avoid RSI.[7,8] Nevertheless, a RF tag cannot be attached to small surgical items such as needles. X-ray imaging has been a commonly used method to detect metal in tissues; however, an X-ray technician must be present during surgery, and a radiologist is required to review the film. Macilquham et al. used X-ray imaging to identify lost surgical needles and found that needles less than 20 mm in length were difficult to identify.[11] Additionally, X-ray imaging exposes the patient and medical personnel to radiation and requires the patient to remain under anesthesia while the X-ray is completed and read by a radiologist.[12] Currently, there is no viable universal platform for real-time detection of various RSIs of different sizes and materials during a surgical operation.

A method was developed previously to synthesize calcined porous silica nano- and microshells with a sol−gel reaction using polystyrene beads as templates and tetramethyl orthosilicate (TMOS) as the silica precursor.[13] The technique has been employed to synthesize 500 nm iron-doped silica shells and 2 μm boron-doped silica shells encapsulating perfluoropentane (PFP) as ultrasound contrast agents for an *in vivo* stationary tumor marker.[14−17] Ultrasound tests showed that PFP-filled silica nanoshells have superior performance to soft microbubbles for imaging longevity (several weeks) by color Doppler imaging.

In the present study, poly(methyl 2-cyanoacrylate) (PMCA) thin films containing 2 μm boron-doped silica shells were fabricated. Commercial ultrasound sound imaging systems depict simple differences in acoustic index in B-mode, but they have additional nonlinear imaging modes such as contrast pulse sequencing (CPS) and color Doppler. In color Doppler, only reflected signals shifted in frequency from the incident ultrasound frequency are detected; this signal is sensitive to motion in tissue such as blood flow and expanding gas. When gas filled, the shells can be activated by widely used clinical ultrasound equipment to exhibit strong color Doppler signals. When the 2 μm particles are fractured during cavitation, the resulting increase in isotropic velocities and pressure results in detected Doppler frequency shifts in all directions. Because of the shell fragmentation, a mosaic Doppler signal is generated. The mosaic signal pattern reflects a fluid with a heterogeneous mixture of sound sources moving in different directions, due to different subpopulations of 2 μm particles being fragmented. These ultrasound active films can be used to coat a variety of surgical tools. Synthetic cyanoacrylates have been traditionally used as biodegradable tissue adhesives for efficient wound closure or sealing vascular sutures.[18] Initiated by surface hydroxyl groups, cyanoacrylate monomers undergo anionic polymerization rapidly in air at room temperature, and the polymerization is catalyzed by moisture.[19] Furthermore, cyanoacrylate polymers have low toxicity and a low rate of infection.[20] Fast-curing poly(methyl 2-cyanoacrylate) can bind to a variety of materials such as metal, plastic, and glass. Polymerization of cyanoacrylate films was used to encapsulate silica microshells while sealing ambient air within the hollow space for ultrasound active coating properties.

Cyanoacrylate monomer containing solvent and porous silica microshells were coated on glass slides and surgical needles by dip coating to provide ultrasound active thin films. Umbilical tapes and surgical clips were also coated with PMCA/microshells films for *in vivo* ultrasound testing. After curing, thin PMCA films were formed with a thickness ranging from 5 to 100 μm. The thickness can be controlled by the coating method. The PMCA film encapsulated the microshells while simultaneously adhering the composite material to the surface of glass slides or needles. The polymerization of methyl 2-cyanoacrylate monomer was initiated by the adsorbed water or the hydroxyl groups on the surface of silica. *In vitro* and *in vivo* ultrasound tests showed that the PMCA/microshells films produced a strong color Doppler signal with a good persistence (>6 h), as required for potential applications to *in vivo* surgical tool detection. The strong color Doppler signal is associated with a macrophase separation during film curing to form a surface layer consisting primarily of embedded microshells with cyanoacrylate acting as an adhesive matrix; however, the base of the film consists primarily of cyanoacrylate polymer tightly bound to the glass or metal substrate (Scheme 1). It is thought that polarity differences between the polymer/solvent phase and the dispersed silica phase cause segregation of the silica shells to the surface layer during film polymerization and solvent evaporation at room temperature.

EXPERIMENTAL SECTION

Materials. Tetramethyl orthosilicate (TMOS), N^1-(3-trimethoxysilylpropyl)diethylenetriamine (DETA), and trimethyl borate (TMB) were purchased from Sigma-Aldrich (St. Louis, MO). The 2 μm polystyrene beads were purchased from Polysciences (Warrington, PA). The commercial methyl-2-cyanoacrylate glue (Loctite 430 Super Bonder Instant Adhesive) was purchased from Henkel Corporation (Rocky Hill, CT). Hard stainless steel wires (0.031 in., 305 mm length) were supplied by RF Surgical Systems, Inc. The wires were cut

DOI: 10.1021/acsami.6b10728
ACS Appl. Mater. Interfaces 2017, 9, 1719−1727

into short sections of 2 cm length and bent into curves to simulate surgical needles. Surgical needles (3/8, taper point, 20 gauge) for the *in vivo* test were purchased from Santa Cruz Biotechnology, Inc. (Dallas, TX). The $1^1/_2$ in. 20 gauge hypodermic needles were purchased from BD Medical (Franklin Lakes, NJ). Umbilical tape (1/8, cut into sections with length of 15 cm) was purchased from Jorgensen Laboratories Inc. (Loveland, CO). Titanium surgical clips were purchased from Teleflex Medical (Research Triangle Park, NC).

Silica Microshells Synthesis. The 2 μm calcined boron-doped silica microshells were synthesized by modifying the literature[15] method to improve templating by adding DETA. In brief, 100 mL of 95% ethanol was added into a 500 mL cylindrical flask with a magnetic stir bar, and 5 mL of 2.6% 2.0 μm polystyrene beads was added to the flask. The mixture was stirred at 1200 rpm at room temperature, while 8 mL of 0.2% DETA in ethanol was added to the flask. The mixture was stirred for 1 h before 310 μL of TMOS was added. After 2 h, 15 μL of TMB was added, and the stirring continued for an additional 5 h. The core−shell particles were centrifuged and washed with 95% ethanol and resuspended and washed two more times before drying in air overnight. The dried particles were calcined at 550 °C for 18 h and produced 17.5 mg of 2 μm microshells.

Fabrication of Silica Particle Containing PMCA Films. 10 mg of 2 μm silica microshells was suspended in 1.0 mL of DCM by sonication and vortex mixed to disperse them before 0.5 mL of methyl 2-cyanoacrylate glue was added. The glue/DCM/microshells mixture was coated on glass slides (2 cm × 0.5 cm) by dipping the slides into the liquid mixture. Four groups of glass slide samples were prepared with 1, 2, 3, and 4 cycles of dip-coating, and each group contained five samples. The interval between cycles was 10 min. Needles were coated with the PMCA/microshells film by dipping the needles into the mixture for eight cycles. The glue film was cured in air at room temperature for 24 h. The thickness of the films was measured by a micrometer. Before the ultrasound tests, the films on one side of the glass slides were removed to guarantee that sonographic properties recorded are from a single film. In addition to DCM, ethyl acetate and acetonitrile were also used as solvents to study the relationship between US performance and the dip-coating solvent. The method of coating of surgical clips is the same as coating of surgical needles except that the clips were dip-coated for four cycles. For the coating of umbilical tapes, 1 mL of DCM containing 2 mg of 2 μm silica microshells was added into 0.5 mL of methyl 2-cyanoacrylate glue. The end of the umbilical tape was dipped into the mixture once. The coated section of the umbilical tape is 1.0 cm long from the end. The glue was cured 24 h at room temperature in air.

Optical and Electronic Microscopic Imaging and Contact Angle Measurement. Optical microscopy was used to visualize PMCA/microshell films on needles. Transmission electron microscopy (TEM) analysis of boron-doped microshells was performed with use of a JEOL (JEOL, Tokyo, Japan) ARM200F operated at 200 kV. TEM samples were prepared by suspending calcined silica microshells in ethanol and dropped onto a lacey carbon film grid substrate. Scanning electron microscopy (SEM) images of microshells and films were obtained using a FEI/Philips XL30 FEG ESEM microscope with an accelerating voltage ranging from 1.5 to 10 kV. SEM samples were prepared by depositing microshells or film-coated needles on a carbon tape substrate. Portions of film for analysis were exfoliated by scratching the film with a razor. Combined field emission SEM (FE-SEM) images were obtained using a Sigma 500 FE-SEM (Zeiss, Germany) with an accelerating voltage ranging from 0.8 to 20 kV. FE-SEM samples were prepared with the same procedure employed for the TEM samples. The contact angles of the films on glass slides were measured by analyzing the photograph of the water drop on the films with ImageJ.

***In Vitro* and *in Vivo* Ultrasound Testing.** All *in vitro* and *in vivo* US tests were performed using a Siemens Acuson Sequoia 512 ultrasound machine with the Acuson 15L8 and 4C1 transducers with center frequencies of 7 and 3 MHz, respectively. Software used for analysis of data included SanteDicom Viewer (Athens, Greece) and Microsoft Excel (Redmond, WA). The tests of ultrasound responsive films on glass slides were performed with the samples in a water tank. The 15L8 US transducer was clamped in the water tank with the sample film facing the transducer. The film was imaged with color Doppler ultrasound with a mechanical index (MI) of 1.9, which is the highest MI permitted by FDA for diagnostic ultrasound imaging. The glass slides were kept in water and subjected to continuous ultrasound radiation for 60 min. The color Doppler signals were recorded over several time periods. The attenuating rates of color Doppler signals were studied by measuring the areas of the signals and comparing the areas with that of the initial signals.

In vitro ultrasound testing of glue/particles film coated needles was performed in a plastic box with a dimension of 20 cm × 15 cm × 6 cm. The box was filled with raw chicken livers to simulate organs in a surgical field. A PMCA/microshells film coated needle was placed in the box. The distance between the needle and the top layer of chicken livers was controlled between 0.5 and 6 cm. The ultrasound properties were studied with an ACUSON Sequoia ultrasound system with a 15L8 and a 4C1 transducer.

In vivo US testing of PMCA/microshell film coated needles, umbilical tapes, and surgical clips was performed using female New Zealand white rabbits purchased from Western Oregon Rabbitry and housed individually in a UCSD vivarium facility. They were kept on a 12 h light/dark cycle and given water and Harlan Teklad commercial pellet diet *ad libitum*. All animal protocols were approved by the UCSD Institutional Animal Care and Use Program (IACUC).

Rabbits were anesthetized with isoflurane and placed on a warmed water pad. The abdomen was shaved and depilated. Instruments and materials were cleaned and sanitized, but not sterilized. Gel was placed on the tip of the ultrasound transducer. Once anesthetized, heart rate and SpO2 were monitored via pulse oximetry, and jaw tone, mucous membrane color, and pedal reflexes were also observed. A midline incision was made from the xiphoid process to the groin; the abdominal wall was retracted. Sharp dissection was used to enter the peritoneal cavity; subsequently, needles were randomly placed throughout to simulate a clinical situation in which a needle breaks off a suture and needs to be retrieved. The surgeon used a 15L8 transducer to explore and locate the needle, and ultrasound signals were recorded. PMCA/microshell film coated umbilical tapes and surgical needles were tested with the same method. Once all items were found, imaged, and removed, then retraction of the abdomen was ceased, and the animal was sacrificed immediately following the surgeon's search.

Postprocessing Detection of Film Signal. The films were imaged using the color Doppler imaging mode which may display color signals from the film, vascular blood flow, or movement from the transducer or subject. Videos were saved along with simultaneous B-mode and color Doppler images in compressed DICOM format and were postprocessed to selectively highlight signal from the film. Signal from the film was distinguishable by its persistent Doppler signal with high spatial and temporal heterogeneity collocated with a strong B-mode signal. Spatial heterogeneity was quantified by calculating the maximum magnitude of the spatial gradient across each of the red, green, and blue (RGB) color channels. Persistence was determined by finding pixels with high spatial heterogeneity lasting at least three frames (~0.2 s). Temporal heterogeneity for each pixel was calculated by integrating the difference in RGB colors from frame to frame. Pixels matching all criteria were shown using a green color overlay to distinguish from the Doppler color map. This processed signal (shown in green in the figures) will henceforth be referred to as microshell signal (MSS). These methods were developed in MATLAB R2015a (The MathWorks Inc., Natick, MA).

Signal properties for detection of the film were compared between imaging in B-mode, color Doppler, and MSS. Sixteen video clips from the *in vivo* experiments of film coated needles were used for analysis. 4% of the frames were randomly sampled (n = 69), and a user-defined region of interest (ROI) was drawn around the needle if present. All pixels outside of the ROI were considered background. B-mode signal-to-noise ratio (SNR) was calculated as the ratio of integrated B-mode image intensity inside the ROI vs outside. Color Doppler and MSS SNR were calculated as the ratio of the area of detected signal inside the ROI vs outside. Color Doppler and MSS sensitivity were calculated

DOI: 10.1021/acsami.6b10728
ACS Appl. Mater. Interfaces 2017, 9, 1719−1727

as the area of detected signal inside the ROI divided by the area of the ROI; specificity was calculated as the area of undetected signal outside the ROI divided by the area outside the ROI. SNR was compared between B-mode, Doppler, and MSS using the Kruskal–Wallis test with multiple comparisons. Sensitivity and specificity were compared between Doppler and MSS using the Mann–Whitney U-test. Statistical analyses were performed in MATLAB R2015a.

RESULTS AND DISCUSSION

Synthesis of 2 μm Boron-Doped Silica Microshells. Figure 1 contains the TEM and SEM images of boron-doped

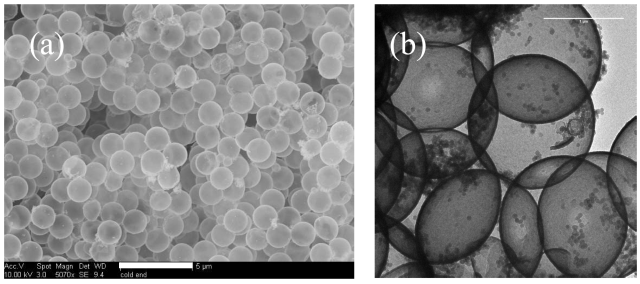

Figure 1. Electron microscopy images of calcined 2 μm boron-doped silica microshells. (a) Scanning electron microscopy (SEM) image. (b) Transmission electron microscopy image. The scale bars in the images are 5 μm (a) and 1 μm (b).

silica microshells. The size and size distribution of the hollow spherical particles were determined from SEM image analysis. The value of the average diameter and standard deviation was 1.71 ± 0.03 μm (n = 20). The thickness of the silica shell wall was determined by TEM image analysis as 30 ± 5 μm (n = 20). The silica shells have a dense, uniform wall with no resolved pore structure, although the porous shell readily permits gases, solvents, and molecules to diffuse in and out. In TEM images, some colloidal silica particles were observed with a diameter of less than 50 nm attached to the surface of the silica microshells.

In the present study, nonmodified 2 μm PS beads were employed as templates, and boron was doped into the silica matrix during the sol–gel condensation to enhance the mechanical strength of the microshells. DETA was used to serve as both the cationic electrolyte and a precursor of silica to better modify the surface of PS beads. The short, positively charged DETA is absorbed to the surface of anionic zeta-potential PS beads, and at the same time the silyl end of DETA was cross-linked by the polycondensation reaction with itself and templated a positively charged surface silica gel network before adding the bulk of TMOS along with trimethyl borate to make the thin silica shell more robust. Since the hydrolysis and polycondensation of trimethy borate are faster than TMOS, it was added 2 h after TMOS addition. The core–shell sol–gel coated microparticles were obtained by centrifugation and calcined at 550 °C to remove the PS cores. Dehydration of the sol gel during calcination resulted in a porous hollow silica gel shell with a diameter smaller than the 2 μm template. Cyanoacrylate glue was used to cross-link silica microshells and bind them to metal or glass surfaces. Loctite 430 was chosen as the cyanoacrylate material because it has low viscosity, which makes it easy to mix with silica shells. The active ingredient is methyl 2-cyanoacrylate which bonds strongly with metals and cures rapidly compared to other synthetic cyanoacrylate adhesives. Organic cosolvents were used to further disperse silica microshells within the glue solution, which lowered the viscosity and slowed curing. The mechanism of the curing of cyanoacrylate glue is by anionic polymerization of cyanoacrylate monomer. The curing of commercial cyanoacrylate glue is initiated when water, a weak base, neutralizes the strong acid inhibitor added to cyanoacrylate glue (Figure 2). For the PMCA/microshells films, the water is likely supplied from the trace amount of water absorbed on the calcined porous silica gel shells.

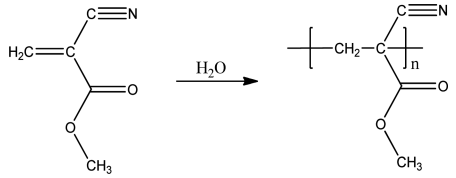

Figure 2. Polymerization of methyl 2-cyanoacrylate. Cyanoacrylate monomers undergo a rapid anionic polymerization on exposure to basic catalysts such as water, which neutralizes the acid inhibitor in commercial cyanoacrylate.

Experiments suggest that water, which initiates the polycondensation of cyanoacrylate, is already adsorbed on the 2 μm silica microshells dispersed in acetonitrile before mixing. For example, two sealed tubes were prepared that were identical, except one omitted the silica microshells. Both samples were cured at room temperature. The viscosity of the glue mixture containing silica shells increased rapidly and turned into a white solid within 24 h. The sample without added silica shells remained liquid for at least 7 days. In another experiment, silica microshells were dried in a glovebox for 24 h at room temperature and then suspended in a glue/acetonitrile solution in a sealed tube. After 24 h, the viscosity of the suspension increased but did not solidify. The same test was performed without drying the silica shells in the glovebox, and the suspension solidified within 24 h. This suggests the water is adsorbed on the silica microshells that were not dried. The hydroxyl groups on the silica shells may play a minor role, but the water absorbed on the shells dominates the curing process.

When the acetonitrile solvent was replaced with DCM, the curing time of glue containing silica microshells was prolonged to 3 days in sealed tubes. This can be attributed to the solubility of water in acetonitrile being much higher than in DCM. Acetonitrile facilitates dissolution of adsorbed water from the silica shells and disperses it into the bulk acetonitrile/cyanoacrylate solution. This initiated the polycondensation much more rapidly than when the water primarily remains adsorbed on the surface of the silica shells in DCM solvent.

The thickness of the PMCA/microshells film can be controlled by varying the concentration of the particles in glue and the number of dip-coating repetition. To test the effect of the number of coating cycles, 20 mg/mL particles in methyl 2-cyanoacrylate were coated onto glass slides with different numbers of repetitions. The film thicknesses on glass slides are 15 ± 3, 31 ± 5, 59 ± 11, and 98 ± 13 μm (five samples each) by dip-coating the slides 1, 2, 3, and 4 times, respectively. Multiple coatings were needed to form a uniform PMCA/microshells film on the needles. A film with a thickness of 18 ± 5 μm was obtained by dip-coating surgical needles eight times each in microshells/glue/DCM mixture; this was replicated for 10 needles. The data are consistent with the surface tension of the round shape of the needle and the surface energy of metal requiring more coatings for the needles. High particle

DOI: 10.1021/acsami.6b10728
ACS Appl. Mater. Interfaces 2017, 9, 1719–1727

concentration produces thicker films after curing as compared to low particle concentrations. When 10 mg/mL particles in methyl 2-cyanoacrylate were coated on needles, a film with a thickness of 8 ± 3 μm was obtained by dip-coating 10 needles eight times each in silica shells/glue/DCM mixture.

***In Vitro* Ultrasound Performance and Macrophase Separation of PMCA/Microshell Films.** Figure 3 displays

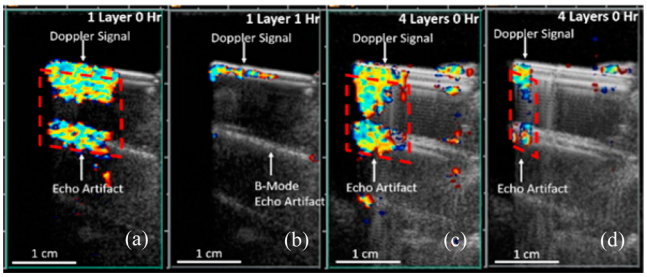

Figure 3. Color Doppler images of silica PMCA/microshells macrophase-separated films on a glass slide. A 15L8 transducer was used, and 7.0 MHz frequency was employed. (a, c) Images of a one- and four-layer film recorded at the beginning of the test, respectively. (b, d) Respective images recorded after the films were exposed to the US for 1 h. The second and third signals below the initial signal are artifacts due to the strong acoustic echo.

the color Doppler signals from PMCA/microshell films on glass slides (blank control in Supporting Information Figure S1). Strong color Doppler signals were observed from films produced by the dip-coating method with DCM as solvent. The broad upper colored image and the secondary image below the signal around the position of glass slides are a known acoustic echo, which is an artifact that is characteristic of very strong color Doppler signals. For such strong imaging, it is likely that the ultrasound pulses release trapped air from the surface microshells to create microbubbles and the strong signal.[21] After prolonged US exposure (Figure 3b,d), the image intensity weakens as the surface layer of microshells releases most of the trapped air.

In the present work, air is used as the contrast agent within the hollow space of silica shells. For microshells in aqueous solution, normally perfluorocarbon gas is necessary for ultrasound activity to prevent gas diffusion/dissolution from the porous microshells and consequent filling of the microshells with water; however, with the polymer coating, simple air filling can be employed since the polymer likely seals the microshell pores. When air-filled 2 μm boron-doped silica microshells were suspended in deionized water without cyanoacrylate coating, no color Doppler signals were observed, indicating that water enters the microshells and dissolves the air. After mixing with methyl 2-cyanoacrylate glue, the macrophase-separated PMCA/microshells persisted for over an hour when exposed to continuous insonation (Figure 3b,d). In another test, PMCA/microshells film coated surgical needles were dipped in a water bath with a temperature of 37 °C for 4 months, and strong color Doppler signals were obtained (Figure S2). This suggests that air was sealed within the shell by the rapid curing of glue on the hydrated silica surface and possibly even in the pores of the silica shells.

Figures 4a and 4b are SEM and STEM images of the surfaces of silica PMCA/microshell films on glass slides. The cyanoacrylate bound clusters of cross-linked shells form a thin, loose, porous 3D network at the surface of the film. It is

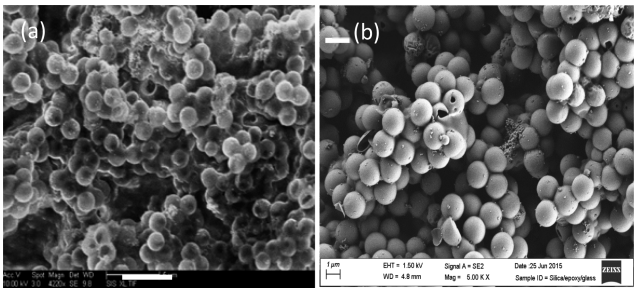

Figure 4. Electron microscopy images of macrophase-separated microshells films. (a) Scanning electron microscopy (SEM) and (b) scanning transmission electron microscopy (STEM) images of a PMCA/microshells film on glass slide. The film was coated on 2 cm stainless steel wires. The scale bars in left and right images are 5 and 2 μm, respectively.

hypothesized that the thin polymer film on the microshells or in their pores blocks the silica gel wall pores and seals air within the hollow space, thereby providing good US contrast performance. The contact angle of the PMCA/microshells film on the glass slide was measured to be 130°, which is consistent with the microshells being covered with a thin hydrophobic polymeric film. The contact angle of PMCA film alone on glass slide is 64°. PMCA is a hydrophobic polymer, and its hydrophobicity increases when the roughness of the surface increases. This was well described in an earlier study.[22]

It was previously reported that perfluorocarbon loaded silica nano- and microshells could give strong color Doppler signals when suspended in water or animal tissues.[15,17,23] Unlike soft microbubble based ultrasound contrast agents, silica shells are rigid and nonelastic. The microshells exhibit a large acoustic impedance mismatch between the surrounding fluid environments. When silica shells are subjected to an ultrasound wave, the shells fracture and release entrapped PFP gas; the released gas is able to expand and contract to generate a nonlinear ultrasound signal.[21] It is hypothesized that the air in the hollow shell worked as the US contrast agent in the cyanoacrylate films. When the PMCA/microshells film was subjected to continuous US waves, the air in the hollow space escaped from the fractured silica shells near the surface so the color Doppler signal attenuates over time. The US signals should not attenuate if the signals were generated just from mismatch of the acoustic response the film surface and surrounding water.

The relationship between the attenuation rate and the thickness of the PMCA/microshells films on glass slides was studied. Figure 5 shows the attenuation rates of color Doppler signals of films with different thicknesses. Note that the intensities were normalized to 1 at time zero. After subjecting the film to continuous US for 1 h, the area of color Doppler signal of all films with different thickness decayed to less than 11% of the initial intensity. With increasing film thickness, the US signals attenuated more slowly, but the effect is small. This indicates that with more dip coating repetitions more silica microshells were deposited on the surface of film, but saturation is quickly reached. It also suggests that only a small fraction of the shells near the surface are releasing gas at any instant in time.

We also compared the intensity of initial US signals of films with different thicknesses (Figure S3). The vertical image length of the color Doppler signal was used to represent the intensity of the US signals. More dip-coating repetitions slightly increased the image size. This is consistent with increased dip-

DOI: 10.1021/acsami.6b10728
ACS Appl. Mater. Interfaces 2017, 9, 1719−1727

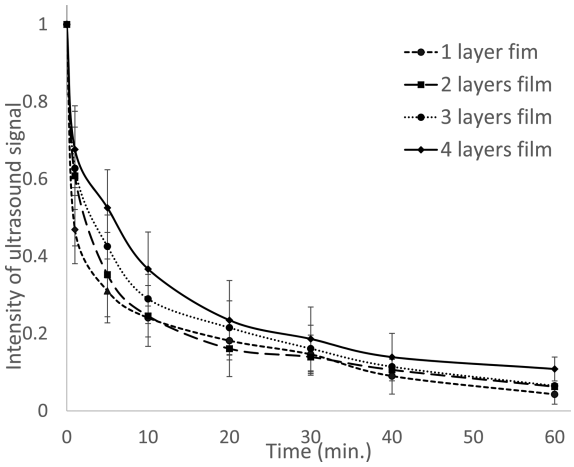

Figure 5. Ultrasound imaging lifetime of macrophase-separated PMCA/microshells films on glass slides. The area of color Doppler signals at specific time periods was imaged and measured and divided by the area of initial signals to approximate the image intensity.

coating repetitions increasing the density of microshells in the surface layer to produce stronger initials signals and slower attenuation. This effect is not dramatic, which suggests only the shells near the surface are US activated. Figure 6a contains an SEM image of a cross section of the PMCA/microshells film coated on the glass slide with DCM as the solvent. The film was exfoliated from the slide for imaging. The flat plate (green arrow) is the polymer film surface, which was proximal to the glass slide, and no silica microshells were observed on this surface. In the cross section, a region of pure polymer matrix and a region composed of polymer and 2 μm shells were clearly observed (separated by red dashed line). On the surface of the film there is another loose layer consisting of mainly 2 μm shells (Figure 4). Three domains present in the film suggest that a macrophase separation occurred during solvent evaporation and polymerization of the cyanoacrylate/microshell composite. When ethyl acetate is employed as solvent, phase separation was also observed in the film, and a US signal was also obtained from the film (Figure S4). To our knowledge, this is the first report of macrophase separation in polymer composites containing hollow inorganic particles. If DCM is replaced with acetonitrile as solvent for the coating, no obvious US signal was imaged from the film on the glass slide. Figure 6b contains an SEM image of the cross section of the film cured with acetonitrile solvent on a surgical needle. No obvious phase separation was found in the cross section (blue arrow). Figure 6c is the SEM image of the front as surface of the film on the surgical needle with acetonitrile as solvent. Only a few silica particles were evident, and no appreciable ultrasound signal was obtained from the film. Phase separation in polymer–nanoparticles composites has been studied previously.[24] Enthalpic and entropic interactions between polymer chains and nanoparticles contribute to phase separation.[25] When polymer chains grow across solid silica particles, they become constrained, which results in loss of conformational entropy. Larger particles are easier to expel from polymers than smaller particles.[26] In the present study, it was observed that phase separation depends on the speed of polymerization of the cyanoacrylate monomer solution, which suggests that macrophase separation may be altered by kinetic control of the curing process. The curing of cyanoacrylate glue is a typical anionic polymerization, and high polarity solvents facilitate more rapid polymerization by producing more free ions as well as aiding the dissolution of adsorbed water (a polymerization aid that reacts with the cyanoacrylate acid inhibitor). Acetonitrile has a

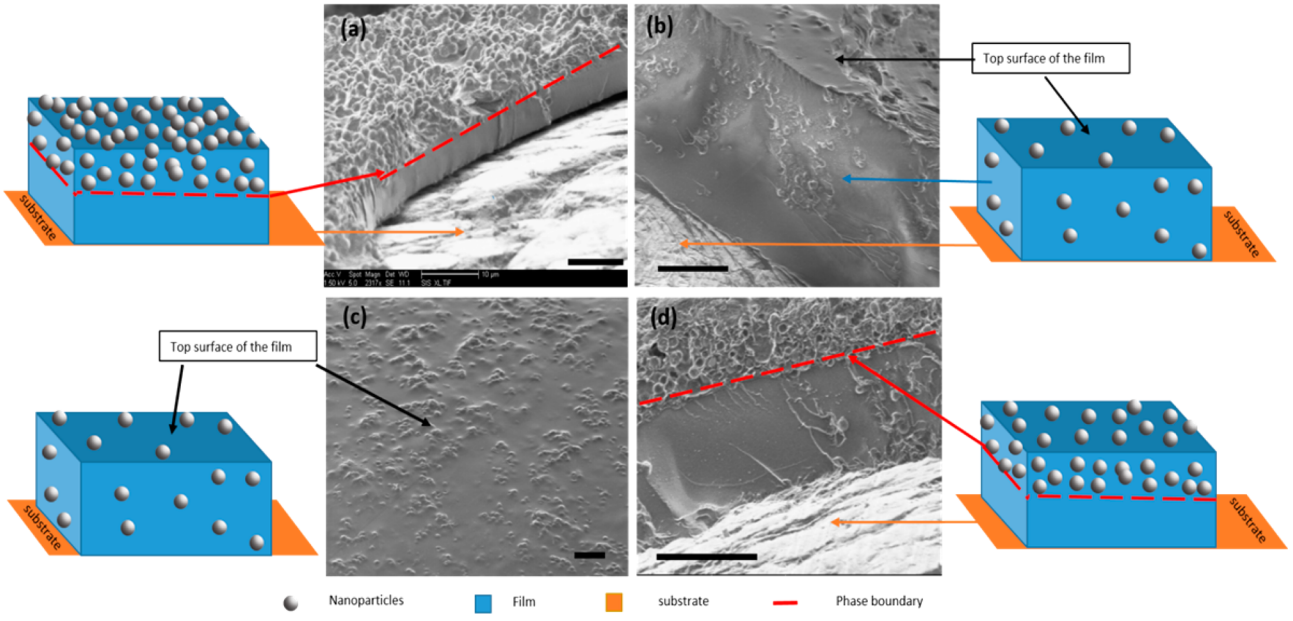

Figure 6. SEM images of cross sections of PMCA/microshells. (a) Cross section of the DCM-based macrophase-separated film which was exfoliated after casting on a glass slide. Red arrow indicates the boundary between the domain of the polymer and the domain of polymer/microshells, and orange arrow indicates the back side of the film against glass slide. (b) Cross section of the acetonitrile-based film coated on a surgical needle. Blue arrow indicates the cross section of the film, black arrow indicates the top surface of the film, and orange arrow indicates the surface of metal needle. (c) Top surface of acetonitrile-based film. (d) Cross section of the acetonitrile-based film on a surgical needle (cured in glovebox). Red arrow indicates the boundary between the domain of the polymer and the domain of polymer/microshells, and orange arrow indicates the metal needle surface. Scale bars in all images are 10 μm.

DOI: 10.1021/acsami.6b10728
ACS Appl. Mater. Interfaces 2017, 9, 1719–1727

high polarity (polarity index is 5.8 compared to that of DCM at 3.1), and the curing of cyanoacrylate is faster in acetonitrile solvent than in DCM and ethyl acetate. Hydrophilic acetonitrile may carry cyanoacrylate monomer through the hydrophilic nanoporous walls of microshells, but the hydrophobicity and viscosity of the DCM/glue mixture make the displacement of air from silica microshells difficult. It is hypothesized that in acetonitrile, when the length of the polymerized chains increases rapidly inside and outside the microshells, the microshells become filled with polymer and trapped within the polymer matrix. After evaporation of solvent, the thick solid polymer matrix makes the microshells nonactivable to US waves.

With DCM or ethyl acetate as solvent, the curing is slower than with acetonitrile; therefore, microshells are driven out of the matrix of short chains of polymer during curing to obtain a thermodynamically favored macrophase-separated composite. With DCM as a solvent, less polar DCM might not be able to efficiently carry monomers through the polar nanopores of the microshells. Slow curing also maintains the glue−solvent mixture at a low viscosity for long time periods, which allows the microshells to phase segregate. At the same time, there is a thin polymer film coating and binding the air-filled surface silica microshells. This coating is too thin to block the ultrasound wave but sufficiently thick to seal the pores of silica shell, thereby allowing the microshells to retain trapped air in the hollow space as ultrasound contrast agent for long time periods.

While the films with phase-separated microshells surface layers gave strong color Doppler signals, no US signals were imaged when the film was a uniform single phase, and the shells were embedded deeper in the polymer matrix. Few 2 μm microshells are observed in the cross section of the single phase film with acetonitrile as solvent (Figure 6b). We assume that the polycyanoacrylate filled in the hollow space of these microshells and air was expelled. The film with two partially separated domains (ethyl acetate solvent) also gave color Doppler signals, but they attenuated quickly and were not as strong as for the film (DCM solvent) with the dense microshell surface layer. The data are consistent with only the microshells near the surface of the film being activated by US waves.

The relationship between the phase separation and the speed of polymerization was further probed by coating PMCA/microshells films on surgical needles in a glovebox filled with nitrogen with acetonitrile as the polymerization solvent. Without atmospheric moisture, cyanoacrylate curing in acetonitrile is significantly slower, allowing enough time for macrophase separation during the retarded polymer chain elongation process. Figure 6d shows the obvious macrophase separation in the film, and color Doppler signals were readily obtained from this film. In the glovebox, trace moisture to initiate polymerization could only come from water initially adsorbed on the silica microshells, and the polymerization of cyanoacrylate was much slower than when air curing the dip-coated films. Extremely slow curing allows the microshells time to phase segregate. When the microshells are close to the surface of film, air may diffuse into the hollow space while cyanoacrylate monomer and oligomer are partly carried out of the microshells with the evaporating solvent. A macrophase separation was thereby obtained by the slower polymerization process. The film is also ultrasound active, but not as active as those cast using DCM solvent.

It also was found that the phase separation depended on the concentration of microshells in cyanoacrylate glue. When 10 mg/mL particles in methyl 2-cyanoacrylate/DCM were dip-coated onto needles with four repetitions, no obvious polymer domain was observed. In SEM and STEM images, the cross section of the film is analogous to the microshells/polycyanoacrylate layer in the phase-separated film; however, there is no loose microshells surface layer (Figure S5). Strong color Doppler US signals were obtained from the film, but the signals attenuated rapidly. This suggests that the macrophase separation did not occur because the polycyanoacrylate chains were less constrained in solutions containing a lower concentration of microshells than in solutions containing the high concentration of microshells. It should be noted that solvent plays a role, since the non-phase-segregated films with rapidly attenuating color Doppler properties were obtained from DCM solvent. The inactivity of films prepared from acetonitrile can be attributed to loss of gas and filling of the microshells with polymer. Such films are optically clear, in contrast to the white opaque films containing gas-filled shells.

To test the PMCA/microshells film as a multipurpose marker for surgical tools, coated needles were hidden in animal organs and located with a clinical ultrasound machine. Figure 7a displays the color Doppler image of a coated 18 mm (3/8 curved) needle in pork liver obtained with a 15L8 transducer with a US center frequency of 7 MHz. The needle is coplanar parallel with the plane of ultrasound waves. Strong color Doppler signals were observed, and the needle was very easily identified against the background. From the scale bar on the side of the image, the depth of the needle in pork liver can be confirmed as about 0.5 cm. The size of the signal is larger than the diameter of the needle because of the strong acoustic echo. Figure 7b displays the ultrasound image of the same needle, but the needle is perpendicular to the plane of ultrasound waves. The bright spot shows only the cross section of the needle, and the dark tail extending down from the needle is the B-mode acoustic echo of the needle due to the strong signal. The color Doppler signal of needles did not significantly attenuate after remaining in the liver tissue for 6 h (without continuous imaging), which indicates that tissue or blood has little effect on degrading the film's image intensity.

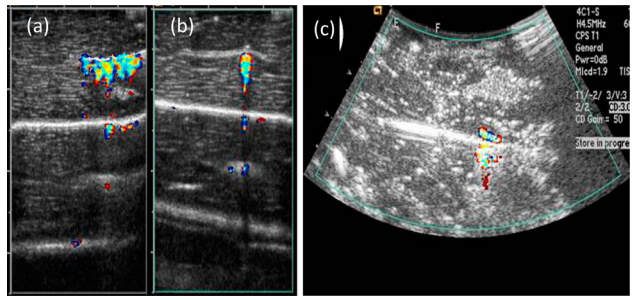

Figure 7. Color Doppler images of macrophase-separated PMCA/microshells film coated 18 mm needle in pork liver. (a) In-plane view of needle imaged with 15L8 transducer and an US frequency of 7 MHz. (b) Cross-sectional view of the needle imaged with 15L8 transducer and an US frequency of 7 MHz. The image sizes are larger than the needle due to the strong ultrasound signal. (c) In-plane view of needle using a 4C1 transducer and an US frequency of 3 MHz.

Figure 7c displays the ultrasound image of a coated 18 mm (3/8 curved) needle in a plastic box filled with chicken livers to mimic an organ cavity environment. The image was obtained with a 4C1 transducer with a center frequency of 3 MHz so that a deeper image could be obtained. The needle was easily

DOI: 10.1021/acsami.6b10728
ACS Appl. Mater. Interfaces 2017, 9, 1719−1727

identified by its strong color Doppler signal. The white stripe between the signal of the needle and its shadow is the acoustic echo from the bottom of the box. The needle was about 5 cm from the top of the box containing densely packed livers. The low-frequency transducer can penetrate deeper in animal tissues than the high-frequency transducer, although the latter displays better spatial resolution.

***In Vivo* Ultrasound Test.** Figure 8 shows the color Doppler images of PMCA/microshells coated surgical needle, umbilical tape, and a surgical clip in the abdomen of a live rabbit. The images were obtained with a 15L8 transducer and a US center frequency of 7 MHz. These surgical tools were covered by organs such as intestines, liver lobes, bladder, or spleen. As shown in Figure 8, the coated surgical items exhibited strong color Doppler signals and could be easily located. PMCA/microshells coated surgical needles gave strong color Doppler signals when the needle is coplanar parallel with the plane of ultrasound waves (Figure 8a). Since the needles have very small surface areas and the lost needles could be at any angle to the transducer, aligning the needles and the plane of ultrasound waves to ensure parallel geometry can be challenging with only a 2D ultrasound transducer. When the tiny needle is perpendicular to the plane of ultrasound waves, it has the smallest surface area exposed to the insonation. Figure 8b shows the color Doppler signals of a needle that is perpendicular to the ultrasound waves. The signals are strong and allow for the needle to be easily located within the tissue. The images of needles parallel and perpendicular to the plane of ultrasound waves are similar to the images obtained during the *in vitro* test, which shows that the living animal tissue environment did not have prevent ultrasound detection. Figures 8c and 8d are images of a coated, cotton umbilical tape and a coated standard surgical clip in the abdomen of a rabbit. The color Doppler signals are very strong due to the relatively larger surface area and increased amount of silica shells that can be activated by the ultrasound waves when compared to the much smaller surgical needles. Alignment of the US transducer is much easier for imaging the items larger than surgical needles.

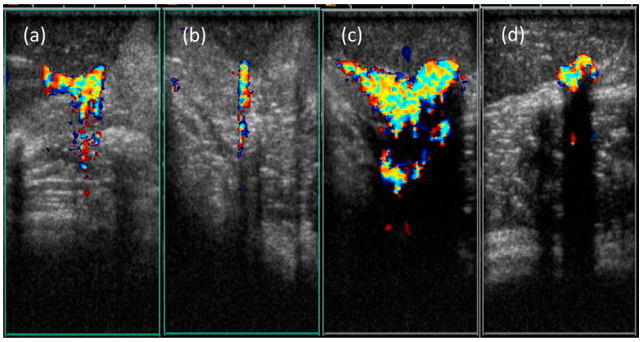

Figure 8. Color Doppler signals of macrophase-separated PMCA/microshells film coated surgical tools in a live rabbit. Surgical needles (a, b), umbilical tape (c), and surgical clip (d) in the abdomen of a live rabbit, imaged with the 15L8 transducer and US frequency of 7 MHz.

To improve identification of small items, such as surgical needles, an algorithm was used for image processing to highlight the location of small items for the viewer. The results of the microshells signal detection algorithm described in the Experimental Section are shown in Figure 9 where the detected processed microshell signal (MSS) is shown as a green overlay in Figure 9c. This is an *in situ* technology to differentiate the film's signals from background noise and possible interfering signals from vessels or other organs and make the searching and locating of medical devices fast and accurate. This is important for minimizing training costs and the use of operating room time. The Doppler and MSS signal data and signal-to-noise ratios (SNRs) are provided in the Supporting Information.

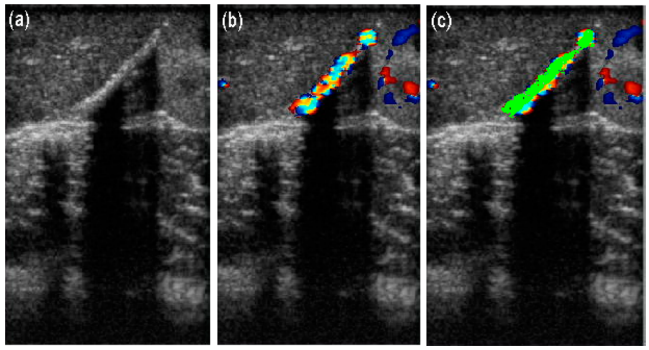

Figure 9. Postprocess video of *in vivo* imaging of macrophase-separated PMCA/microshells film coated 790 nm diameter stainless steel wire with 15L8 transducer and an US frequency of 7 MHz. Videos for the coated wire in the abdomen of a live rabbit were postprocessed to specifically highlight signal from the microshells by detecting areas of (a) strong B-mode signal with persistently high spatial and (b) temporal heterogeneity in the simultaneous color Doppler image. (c) The green overlay indicates where the algorithm identified a microshells signal (MSS), which is double positive for B-mode and color Doppler signal intensity.

CONCLUSION

Ultrasound imaging is a noninvasive, nonradioactive, and low-cost technology for diagnosis and identification of implantable medical devices in real time. New ultrasound activated coatings are important to broaden the utility of *in vivo* marking by improving the accessibility, utility, and accuracy of ultrasound imaging. Ultrasound responsive macrophase-segregated micro-composite thin films were developed to be coated on medical devices composed of multiple materials and with multiple shapes and varying surface areas. The macrophase-segregated films containing 2 μm boron-doped silica microshells in polycyanoacrylate produce strong color Doppler signals with the use of a standard clinical US transducer. Electron microscopy showed a macrophase separation during slow curing of the cyanoacrylate adhesive, as air-filled silica microshells were driven to the surface of the film. The air sealed in the hollow space of the silica shells acted as an ultrasound contrast agent, and echo decorrelation of air exposed to US waves produces color Doppler signals. *In vitro* and *in vivo* tests showed PMCA/microshells film coated needles, umbilical tapes, and surgical clips could be located easily in live animal tissues and organs. This technology demonstrates potential applications of locating and monitoring surgical tools that are deep within a tissue cavity by ultrasound imaging.

ASSOCIATED CONTENT

Supporting Information

The Supporting Information is available free of charge on the ACS Publications website at DOI: 10.1021/acsami.6b10728.

Figure of the intensity of initial color Doppler signals, for the control blank, and for films as the number of

DOI: 10.1021/acsami.6b10728
ACS Appl. Mater. Interfaces 2017, 9, 1719−1727

substrate dip coatings varies, SEM images of 10 mg/mL microshells/cyanoacrylate glue film coated hypodermic needles, ultrasound signals of microshells/PMCA film coated needles dipped in 37 °C water bath for 137 days and ultrasound signals of microshells/PMCA film on surgical needles with ethyl acetate as solvent, tables of cumulative signal properties over all frames, and statistics of signal properties measured frame-by-frame for postprocessing ultrasound signals (PDF)

AUTHOR INFORMATION

Corresponding Authors

*E-mail slblair@ucsd.edu (S.L.B.).
*E-mail akummel@ucsd.edu (A.C.K.).
*E-mail wtrogler@ucsd.edu (W.C.T.).

ORCID

William C. Trogler: 0000-0001-6098-7685

Notes

The authors declare the following competing financial interest(s): A.C. Kummel and W.C. Trogler, scientific cofounders, have an equity interest in Nanocyte Medical, Inc., a company that may potentially benefit from the research results and also serve on the companys Scientific Advisory Board. S. L. Blair has a family member with an equity interest in Nanocyte Medical, Inc., a company that may potentially benefit from the research results. The terms of this arrangement have been reviewed and approved by the University of California, San Diego in accordance with its conflict of interest policies.

ACKNOWLEDGMENTS

Financial support was provided by a grant from RF Surgical Systems Inc. (now a subsidiary of Covidien-Medtronic Inc., Grant agreement #20150893). The authors acknowledge the California Institute for Telecommunications and Information Technology for use of electronic microscopy facilities in the Nano3 cleanroom.

REFERENCES

(1) Sofocleous, C. T.; Schur, I.; Cooper, S. G.; Quintas, J. C.; Brody, L.; Shelin, R. Sonographically Guided Placement of Peripherally Inserted Central Venous Catheters: Review of 355 Procedures. *AJR, Am. J. Roentgenol.* **1998**, *170* (6), 1613−6.

(2) Thomassin-Naggara, I.; Lalonde, L.; David, J.; Darai, E.; Uzan, S.; Trop, I. A Plea for the Biopsy Marker: How, Why and Why Not Clipping after Breast Biopsy? *Breast Cancer Res. Treat.* **2012**, *132* (3), 881−893.

(3) Rönkä, R.; Krogerus, L.; Leppänen, E.; von Smitten, K.; Leidenius, M. Radio-Guided Occult Lesion Localization in Patients Undergoing Breast-Conserving Surgery and Sentinel Node Biopsy. *Am. J. Surg.* **2004**, *187* (4), 491−496.

(4) Ratner, B. D.; Hoffman, A. S.; Schoen, F. J.; Lemons, J. E. *Biomaterials Science: An Introduction to Materials in Medicine*; Academic Press: Cambridge, 2004.

(5) Gray, A. T. Ultrasound-Guided Regional Anesthesiacurrent State of the Art. *Anesthesiology* **2006**, *104* (2), 368−373.

(6) Sites, B. D.; Chan, V. W.; Neal, J. M.; Weller, R.; Grau, T.; Koscielniak-Nielsen, Z. J.; Ivani, G. The American Society of Regional Anesthesia and Pain Medicine and the European Society of Regional Anaesthesia and Pain Therapy Joint Committee Recommendations for Education and Training in Ultrasound-Guided Regional Anesthesia. *Reg. Anesth. Pain Med.* **2010**, *35* (2), S74−S80.

(7) Chapman, G.; Johnson, D.; Bodenham, A. Visualisation of Needle Position Using Ultrasonography. *Anaesthesia* **2006**, *61* (2), 148−158.

(8) Reusz, G.; Sarkany, P.; Gal, J.; Csomos, A. Needle-Related Ultrasound Artifacts and Their Importance in Anaesthetic Practice. *Br. J. Anaesth.* **2014**, *112* (5), 794−802.

(9) Gibbs, V. C. Retained Surgical Items and Minimally Invasive Surgery. *World J. Surg.* **2011**, *35* (7), 1532−1539.

(10) Wan, W.; Le, T.; Riskin, L.; Macario, A. Improving Safety in the Operating Room: A Systematic Literature Review of Retained Surgical Sponges. *Curr. Opin. Anaesthesiol.* **2009**, *22* (2), 207−214.

(11) Macilquham, M. D.; Riley, R. G.; Grossberg, P. Identifying Lost Surgical Needles Using Radiographic Techniques. *AORN J.* **2003**, *78* (1), 73−78.

(12) Barrow, C. J. Use of X-Ray in the Presence of an Incorrect Needle Count. *AORN J.* **2001**, *74* (1), 80−81.

(13) Yang, J.; Lind, J. U.; Trogler, W. C. Synthesis of Hollow Silica and Titania Nanospheres. *Chem. Mater.* **2008**, *20* (9), 2875−2877.

(14) Liberman, A.; Wu, Z.; Barback, C. V.; Viveros, R.; Blair, S. L.; Ellies, L. G.; Vera, D. R.; Mattrey, R. F.; Kummel, A. C.; Trogler, W. C. Color Doppler Ultrasound and Gamma Imaging of Intratumorally Injected 500 Nm Iron−Silica Nanoshells. *ACS Nano* **2013**, *7* (7), 6367−6377.

(15) Martinez, H. P.; Kono, Y.; Blair, S. L.; Sandoval, S.; Wang-Rodriguez, J.; Mattrey, R. F.; Kummel, A. C.; Trogler, W. C. Hard Shell Gas-Filled Contrast Enhancement Particles for Colour Doppler Ultrasound Imaging of Tumors. *MedChemComm* **2010**, *1* (4), 266−270.

(16) Liberman, A.; Martinez, H. P.; Ta, C. N.; Barback, C. V.; Mattrey, R. F.; Kono, Y.; Blair, S. L.; Trogler, W. C.; Kummel, A. C.; Wu, Z. Hollow Silica and Silica-Boron Nano/Microparticles for Contrast-Enhanced Ultrasound to Detect Small Tumors. *Biomaterials* **2012**, *33* (20), 5124−5129.

(17) Liberman, A.; Wang, J.; Lu, N.; Viveros, R. D.; Allen, C.; Mattrey, R.; Blair, S.; Trogler, W.; Kim, M.; Kummel, A. Mechanically Tunable Hollow Silica Ultrathin Nanoshells for Ultrasound Contrast Agents. *Adv. Funct. Mater.* **2015**, *25* (26), 4049−4057.

(18) Leggat, P. A.; Smith, D. R.; Kedjarune, U. Surgical Applications of Cyanoacrylate Adhesives: A Review of Toxicity. *ANZ. J. Surg.* **2007**, *77* (4), 209−213.

(19) Kilpikari, J.; Lapinsuo, M.; Törmälä, P.; Pätiälä, H.; Rokkanen, P. Bonding Strength of Alkyl-2-Cyanoacrylates to Bone in Vitro. *J. Biomed. Mater. Res.* **1986**, *20* (8), 1095−1102.

(20) Toriumi, D. M.; Raslan, W. F.; Friedman, M.; Tardy, M. E. Histotoxicity of Cyanoacrylate Tissue Adhesives: A Comparative Study. *Arch. Otolaryngol., Head Neck Surg.* **1990**, *116* (5), 546−550.

(21) Ta, C. N.; Liberman, A.; Martinez, H. P.; Barback, C. V.; Mattrey, R. F.; Blair, S. L.; Trogler, W. C.; Kummel, A. C.; Wu, Z. Integrated Processing of Contrast Pulse Sequencing Ultrasound Imaging for Enhanced Active Contrast of Hollow Gas Filled Silica Nanoshells and Microshells. *J. Vac. Sci. Technol., B: Nanotechnol. Microelectron.: Mater., Process., Meas., Phenom.* **2012**, *30* (2), 02C104.

(22) Levkin, P. A.; Svec, F.; Fréchet, J. M. Porous Polymer Coatings: A Versatile Approach to Superhydrophobic Surfaces. *Adv. Funct. Mater.* **2009**, *19* (12), 1993−1998.

(23) Kang, S.-T.; Lin, J.-L.; Wang, C.-H.; Chang, Y.-C.; Yeh, C.-K. Internal Polymer Scaffolding in Lipid-Coated Microbubbles for Control of Inertial Cavitation in Ultrasound Theranostics. *J. Mater. Chem. B* **2015**, *3* (29), 5938−5941.

(24) Zou, H.; Wu, S.; Shen, J. Polymer/Silica Nanocomposites: Preparation, Characterization, Properties, and Applications. *Chem. Rev.* **2008**, *108* (9), 3893−3957.

(25) Balazs, A. C.; Emrick, T.; Russell, T. P. Nanoparticle Polymer Composites: Where Two Small Worlds Meet. *Science* **2006**, *314* (5802), 1107−1110.

(26) Wells, G.; De Borst, R.; Sluys, L. A Consistent Geometrically Non-Linear Approach for Delamination. *Int. J. Numer. Methods Eng.* **2002**, *54* (9), 1333−1355.

DOI: 10.1021/acsami.6b10728
ACS Appl. Mater. Interfaces 2017, 9, 1719−1727